

Dynamic Reconfiguration of Mission Parameters in Underwater Human-Robot Collaboration

Md Jahidul Islam¹, Marc Ho², and Junaed Sattar³ *

June 19, 2022

Abstract

This paper presents a real-time programming and parameter reconfiguration method for autonomous underwater robots in human-robot collaborative tasks. Using a set of intuitive and meaningful hand gestures, we develop a syntactically simple framework that is computationally more efficient than a complex, grammar-based approach. In the proposed framework, a convolutional neural network is trained to provide accurate hand gesture recognition; subsequently, a finite-state machine-based deterministic model performs efficient gesture-to-instruction mapping, and further improves robustness of the interaction scheme. The key aspect of this framework is that it can be easily adopted by divers for communicating simple instructions to underwater robots without using artificial tags such as fiducial markers, or requiring them to memorize a potentially complex set of language rules. Extensive experiments are performed both on field-trial data and through simulation, which demonstrate the robustness, efficiency, and portability of this framework in a number of different scenarios. Finally, a user interaction study is presented that illustrates the gain in usability of our proposed interaction framework compared to the existing methods for underwater domains.

1 Introduction

A simple yet robust human-robot communication framework [1–3] is desired in many tasks which would require the use of autonomous underwater vehicles (AUVs). Particularly, the ability to recognize direct human guidance and instructions during task execution (see Fig. 1) is of vital importance, as truly autonomous

*The authors are with the Department of Computer Science and Engineering, University of Minnesota-Twin Cities, MN 55455, USA.

E-mail: {¹islam034, ²hoxxx323, ³junaed}@umn.edu

underwater navigation is still an open problem, with the underwater domain posing unique challenges to robotic sensing, perception, construction, and manipulation. Additionally, such semi-autonomous behavior of a mobile robot with human-in-the-loop guidance reduces operational overhead by eliminating the necessity of tele-operation (and a tele-operator). However, simple and intuitive instruction sets and robust instruction-to-action mapping are essential for successful use of AUVs in a number of critical applications such as search-and-rescue, surveillance, underwater infrastructure inspection and marine ecosystem monitoring.

The ability to alter parts of instructions, *i.e.*, modifying subtasks in a larger instruction set, and reconfiguring program parameters are often important for underwater exploration and data collection processes. Because of the specific challenges in the underwater domain, what would otherwise be straightforward deployments in terrestrial settings often become extremely complex undertakings for underwater robots, which require close human supervision. Since WiFi or radio (*i.e.*, electromagnetic) communication is not available or severely degraded underwater [4], such methods cannot be used to instruct an AUV to dynamically reconfigure command parameters. The current task thus needs to be interrupted, and the robot needs to be brought to the surface, in order to reconfigure its parameters. This is inconvenient and often expensive in terms of time and physical resources. Therefore, triggering parameter changes based on human input while the robot is underwater, and without requiring a trip to the surface, is a simpler and more efficient alternative approach.

Controlling a robot using speech, direct keyboard or joystick input, or free-form gestures is a general paradigm [5–7] in the context of Human-Robot Interaction (HRI). Unlike relatively less challenging terrestrial environments, the use of keyboard or joystick interfaces or tactile sensors is unappealing in underwater applications since it entails costly waterproofing and introduces an additional point of failure. Additionally, since speech or RGB-D (*i.e.*, visual and depth image)-based interfaces, such as a Leap Motion™ or Kinect™ are not feasible underwater, vision-based communication schemes are more natural for diver-robot interaction.

This work explores the challenges involved in designing a hand gesture based human-robot communication framework for underwater robots. In particular, a simple interaction framework is developed where a diver can use a set of *intuitive* and meaningful hand gestures to program the accompanying robot or reconfigure program parameters on the fly. A convolutional neural network based robust hand gesture recognizer is used with a simple set of gesture-to-instruction mapping. A finite-state machine based interpreter ensures predictable robot behavior by eliminating spurious inputs and incorrect instruction compositions.



Figure 1: Divers programming an AUV using the RoboChat [1] language using ARTag [8] markers. Note the thick “tag book” being carried by the diver, which, while necessary, adds to the diver’s cognitive load and impacts mission performance

2 Related Work

Modulating robot control based on human input in the form of speech, hand gestures, or keyboard interfaces, has been explored extensively for terrestrial environments [5–7, 9]. However, most of these human-robot communication modules are not readily applicable in underwater applications due to environmental and operational constraints [4]. Since visual communication is more feasible and operationally simpler, a number of visual diver-robot interaction frameworks have been developed in the literature.

A gesture-based framework for underwater visual-servo control was introduced in [10], where a human operator on the surface was required to interpret the gestures and modulate robot movements. Due to challenging visual conditions underwater [4] and lack of robust gesture recognition techniques, use of fiducial markers became popular as they are efficiently and robustly detectable under noisy conditions. In this regard, most commonly used fiducial markers have been those with square, black-and-white patterns providing high contrast, such as ARTags [8] and April Tags [11], among others. These consist of black symbols on a white background (or the opposite) in different patterns enclosed within a square. Circular markers such as the Photomodeler Coded Targets Module system [12] and Fourier

Tags [13] have also been used in practice.

RoboChat [1] is the first visual language proposed for underwater diver-robot communication. Divers use a set of ARTag markers to display predefined sequences of symbolic patterns to the robot, though the system is independent of the exact family of fiducial markers that are being used. These symbol sequences are mapped to a set of grammar rules defined for the language. These grammar rules include both terse imperative action commands as well as complex procedural statements. Despite its utility, RoboChat suffers from two critical weaknesses. Firstly, because a separate marker is required for each *token* (*i.e.*, a language component), a large number of marker cards need to be securely carried over to the operation, manually searched for the right ones to formulate a syntactically correct script; this whole process involves high cognitive load on the diver. Secondly, the symbol-to-instruction mapping is inherently unintuitive, which makes it inconvenient for rapidly programming a robot in real-time. The first limitation is addressed in [2], where a set of discrete motions using a pair of fiducial markers are interpreted as robot commands. Different features such as shape, orientation, and size of these gestures are extracted from the observed motion and mapped to the robot instructions. Since more information is embeddable in each trajectory, a large number of instructions can be supported using only two fiducial markers. However, it introduces additional computational overhead to track the marker motion, needs robust detection of shape, orientation, and size of the motion trajectory, and the problems are exacerbated as both robot and human are suspended in a six-degrees-of-freedom (6DOF) environment. Furthermore, the symbol-to-instruction mapping remains unintuitive.

Since the traditional method for communication between scuba divers is with hand gestures, instructing robot using hand gestures offers more intuitiveness and flexibility than using fiducial markers. Additionally, it relieves the divers of the task of carrying a set of markers, which if lost, would put the mission in peril. There exists a number of robust hand gesture based HRI frameworks [5–7, 14] for terrestrial robots. In addition, recent visual hand gesture recognition techniques [15–17] based on convolutional neural networks have been shown to be highly accurate and robust to noise and visual distortions. A number of such visual recognition and tracking techniques have been successfully used for underwater tracking [18] and have proven to be more robust than other purely feature-based methods (*e.g.*, [19]). However, feasibility of these models for hand gesture based diver-robot communication has not been explored in-depth yet.

3 Methodology

The proposed framework is built on a number of components: the choice of hand gestures to map to command tokens, the robust recognition of hand gestures, and the use of a finite-state machine to enforce command structure and ignore erroneous detections or malformed commands. Each of these components are described in detail in the following sections.

3.1 Mapping Hand Gestures to Language Tokens

The key objective of this work is to design a simple, yet expressive framework that can be easily adopted by divers for communicating instructions to the robot without using fiducial markers or memorizing complex language rules. Therefore, we choose a small collection of visually distinctive and intuitive gestures, which would improve the likelihood of robust recognition in degraded visual conditions. Specifically, we use only the ten gestures shown in Fig. 2.

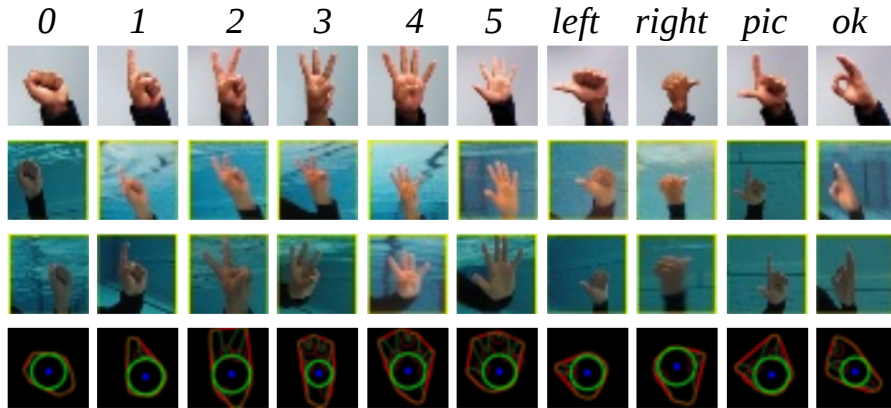


Figure 2: The first three rows show sampled training images for ten different hand gestures in separate columns. The bottom row shows expected hand-contour with different curvature markers for each gesture.

As seen from Fig. 2, each hand gesture is intuitively associated with the command it delivers. Sequences of different combinations of these gestures formed with both hands are mapped to specific instructions. This work concentrates on two different sets of instructions as illustrated in Fig. 3, which are in the following form:

- **Task switching:** This is for instructing the robot to stop executing the current program and start a task specified by the diver, such as hovering, fol-

lowing, or moving left/right/up/down, etc. In other words, these commands are atomic behaviors that the robot is capable of executing. An optional argument can be provided to specify the length of time for the new task (in seconds). Another task-switching operation is to stop executing the current program and start another one; the difference here is that the robot switches from one sequence of instructions to another set of instructions, not just an atomic behavior. An operational requirement is that desired programs need to be numbered and known to the robot beforehand.

- **Parameter reconfiguration:** This is to instruct the robot to continue the current program with updated parameter values. This enables underwater missions to continue unimpeded (as discussed in Section 1), without interrupting the current task or requiring the robot to be brought to the surface. Here, the requirement is that the tunable parameters need to be numbered and their choice of values need to be specified beforehand. The robot can also be instructed to take pictures (for some time) while executing the current program. This is important for underwater missions, as this facilitates visual scene logging as the robot executes a preset mission (also, other sensory data can easily be logged in the same mechanism through a simple extension of the command triggered by a gesture).

The proposed framework supports a number of task switching and parameter reconfiguration instructions, which can be extended to accommodate more by simply changing or appending a user-editable configuration file. The hand gesture-to-token mapping is carefully designed so that the robot formulates executable instructions only when intended by the diver. This is done by attributing specific hand gestures as *sentinels* (i.e., *start-* or *end-tokens*). Fig. 4 illustrates the gesture to micro-instruction mapping used in our framework. Additional examples are shown in Fig. 5, where series of (*start_token*, *instruction*, *end_token*) tuples are mapped to corresponding sequences of *gesture_tokens*.

3.2 Hand Gesture Recognition and Instruction Generation

Any human-robot communication method must be able to recognize individual tokens robustly, independent of the modality used (e.g., aural, tactile or visual). In the proposed framework, the challenges lie in segmenting the hand gestures from the camera image, accurate recognition of hand gestures, and then mapping the gestures to instructions. Fig. 6 illustrates the overall process, and the implementation details of each computational component of our framework is described in the following sections.

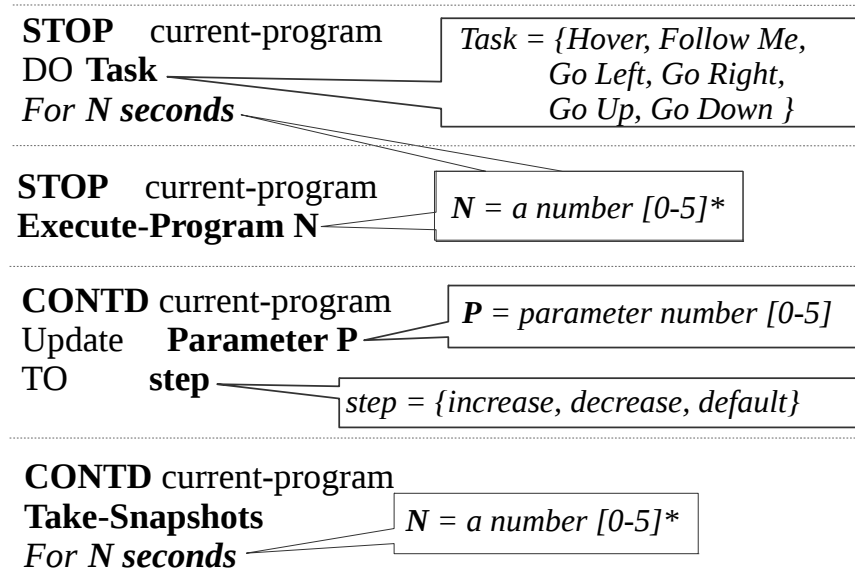


Figure 3: Set of *task switching* and *parameter reconfiguration* instructions that are currently supported by our framework

3.2.1 Region Selection

To detect gestures, the hand regions need to be cleanly extracted from the image, which can be challenging in noisy or degraded visual conditions underwater. These regions are rectangular but vary in size as divers can be at different distances from the robot. One possible approach is to slide a rectangular window at multiple scales sequentially over the image and attempt hand detections; however, trying out each possible rectangular region in such a brute-force fashion is not feasible due to computational and real-time operational constraints. Instead, the following approach is adopted:

1. First, the camera image (in RGB space) is blurred and thresholded in HSV-space for skin-color segmentation [20]. Here, we assume the diver performs gestures with bare hands; if the diver is to wear gloves, the color thresholding range in the HSV space needs to be adjusted accordingly.
2. Then, contours of the different segmented regions in the filtered image-space are extracted (see Fig. 7). Subsequently, different contour properties such as



































Instruction-token	Type	Hand gestures		Gesture-token {left, right}
		Left	Right	
STOP current-program	Start-token			{0, ok}
HOVER	Task			{5, 5}
FOLLOW me	Task			{5, 1}
Go LEFT	Task			{0, left}
Go RIGHT	Task			{0, right}
Go UP	Task			{right, right}
Go DOWN	Task			{left, left}
EXECUTE Program	Task			{pic, 2}
CONTD current-program	Start-token			{pic, 0}
Take SNAPSHOT	Task			{pic, pic}
N (number)	[0-5]*			{ok, 0-5}
P (parameter number)	[0-5]*			{0-5, pic}
next_digit	indicator			{pic, ok}
Increase	step			{right, pic}
Decrease	step			{left, pic}
Default	step			{ok, pic}
GO	End-token			{ok, ok}

Figure 4: Mapping of gesture-token to instruction-token used in our framework

convex hull boundary and center, convexity defects, and important curvature points are extracted. We refer to [21] for details about properties and significance of these contour properties.

3. Next, outlier regions are rejected using cached information about the scale and location of hand gestures detected in the previous frame. This step is of course subject to availability of the cached information.
4. Finally, the hand-contours of potential regions are matched with a bank of hand-contours that are extracted from training data (one for each class of hand gestures as shown in the bottom row of Fig. 2). Final regions for left and right hand gestures are selected using the proximity values of the closest contour match [21]; *i.e.*, region that is most likely to contain a hand gesture is selected.





















<i>Instruction:</i>	STOP current-program, HOVER For 50 seconds, GO.	
<i>Gesture-tokens:</i>	 {0, ok}	 {5, 5}
	<i>{start_token}</i>	<i>{task}</i>
	 {ok, 5}	 {pic, ok}
	 {ok, 0}	 {ok, ok}
	<i>{number}{next_digit}{number}</i>	<i>{end_token}</i>
<i>Instruction:</i>	CONTD current-program, take SNAPSHOTS For 20 seconds, GO.	
<i>Gesture-tokens:</i>	 {pic, 0}	 {pic, pic}
	 {ok, 2}	 {pic, ok}
	 {ok, 0}	 {ok, ok}
<i>Instruction:</i>	CONTD current-program, Update Parameter 3 TO DECREASE , GO.	
<i>Gesture-tokens:</i>	 {pic, 0}	 {3, pic}
	 {left, pic}	 {ok, ok}
<i>Instruction:</i>	STOP current-program, EXECUTE Program 1 , GO.	
<i>Gesture-tokens:</i>	 {0, ok}	 {pic, 2}
	 {ok, 1}	 {ok, ok}

Figure 5: Some examples of different combinations of hand gestures which are used to generate instructions (based on the gesture-instruction mapping shown in Fig. 4)

3.2.2 CNN Model for Gesture Recognition

Following region selection, cropped and resized image-patches of 32×32 are fed to a convolutional neural network (CNN) for gesture recognition. The detailed architecture of the model is illustrated in Fig. 9. Two convolutional layers are used for extracting and learning the spatial information within the images. Spatial down-sampling is done by max-pooling, while the normalization layer is used for scaling and reentering the data before feeding it to the next layer. The extracted feature vectors are then fed to fully connected layers to learn decision hyperplanes within the distribution of training data. Finally, a soft-max layer provides output probabilities for each class, given input data. Note that similar CNN models have been shown to perform well for small-scale (*i.e.*, 10-class classification) problems [22], which is similar to our problem.

Dimensions of each layer and number of parameters are specified in Fig. 9; details about training and data-sets are provided in Section 4. The trained model is used for classifying hand gestures on 32×32 image patches provided by the *region selection* step. The classified gesture-tokens are passed to a Finite-State Machine (FSM)-based gesture-to-instruction decoder, which we discuss next.

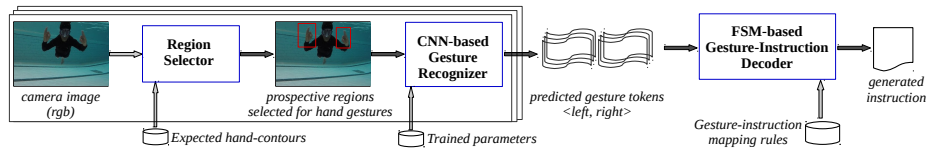


Figure 6: Overview of the process to map hand gestures to instructions, left to right. The left half demonstrates the CNN-based recognition system, whereas the right half depicts the finite-state machine for robust mapping of gestures to instructions.

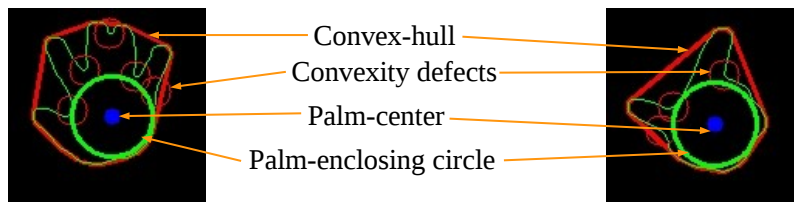


Figure 7: Two examples of hand-contours including different contour properties; the left image corresponds to gesture ‘5’ while the right image corresponds to gesture ‘pic’.

3.2.3 FSM-based Gesture to Instruction Decoder

An FSM-based deterministic model is used for efficient gesture-to-instruction mapping. As illustrated in Fig. 10, the transitions between instruction-tokens are defined as functions of gesture-tokens based on the rules defined in Fig. 4. Here, we impose an additional constraint that each gesture-token has to be detected for 15 consecutive frames for the transition to be activated. This constraint adds robustness to missed or wrong classification for a particular gesture-token. Additionally, it helps to discard noisy tokens caused when diver changes from one hand gestures to the next. Furthermore, since the mapping is one-to-one, it is highly unlikely that a wrong instruction will be generated even if the diver mistakenly performs some inaccurate gestures because there are no transition rules other than the correct ones at each state.

4 Experimental Results

Now we present the experimental results and discuss related implementation details of the proposed framework.

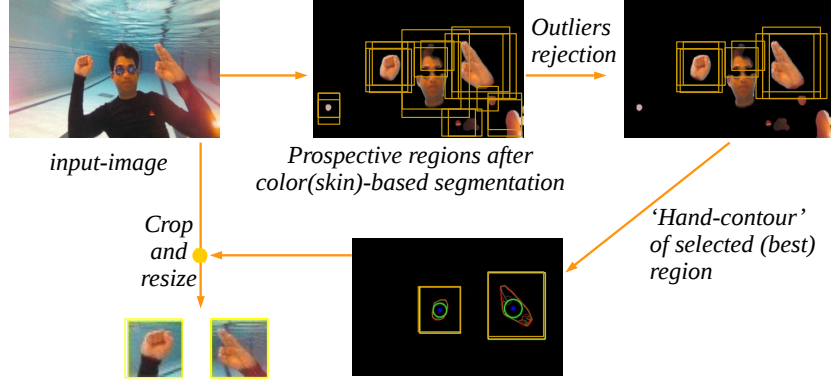


Figure 8: Outline of the region selection mechanism of our framework. First, the color(skin)-based segmentation is performed to get potential regions for hand gestures; then, outliers are discarded based on cached information about previous location of the hands.

4.1 Training the CNN Model

The CNN model is implemented using TensorFlow [23] and trained on a Linux machine (CPU) over 35K rgb-images of hand gestures (3.5K for each class). Training data contain $32 \times 32 \times 3$ images from both underwater and terrestrial environments. A few samples from the training images are shown in Fig. 2 and details about our CNN model are provided in Fig. 9. Additional 4K images are used for validation and a separate 1K images are used as a test-set.

It takes about a couple of hours to train the model over 50 epochs while it reaches a training accuracy of 0.997. Once the network is trained, model parameters are saved, which is loaded later during testing to perform inference. Fig. 11 illustrates the learning behavior of the network in terms of training loss and classification accuracy. Maximum validation accuracy of 0.986 is achieved after 50 epochs of training, and the test-set accuracy is 0.969. Fig. 12 shows the confusion matrix based on test-set performance of the model.

4.2 Performance Evaluation on Real-World Data

We used an underwater drone (OpenROV 2.8 [24]) for our experiments in a closed-water (swimming pool) scenario. Sequences of hand gestures pertaining to different types of instructions are performed by three participants. In addition, synthetic test-data is generated by augmenting different combinations of the recorded

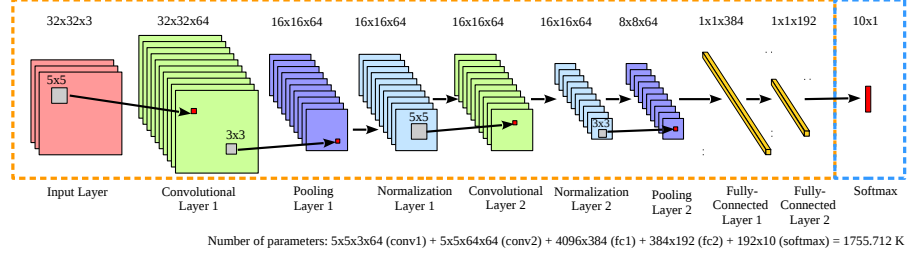


Figure 9: Architecture of the CNN model used in our framework for hand gesture recognition

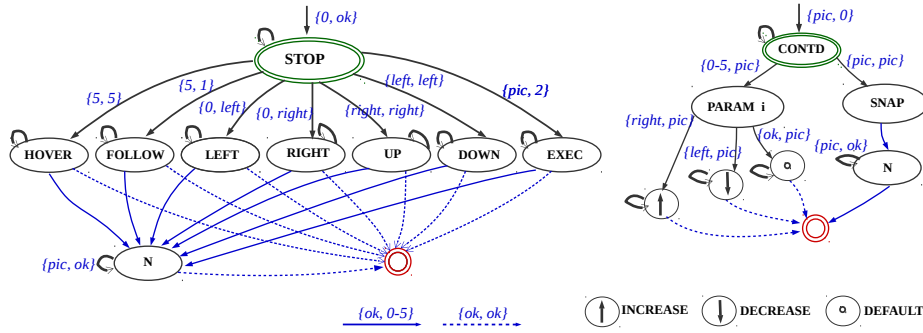


Figure 10: FSM-based deterministic mapping of gestures-to-instructions (based on the rules defined in Fig. 4)

gesture-sequences.

The test data is used to evaluate the performance our framework, as demonstrated in Fig. 13. There are a total of 30 sets of images-sequences in the test set (each image is $640 \times 480 \times 3$). Additional 20 sets of test-data are collected on land to inspect the performance in noise-free visual conditions. Table 1 summarizes the performance of our framework for both classes of test data. We find that the overall accuracy of the framework mostly depends on region selection; that is, once the hand gestures are correctly segmented out, gesture recognition and gesture-to-instruction mapping are mostly accurate. As demonstrated by the bottom row of Table 1, our framework successfully decoded all instructions from the noise-free terrestrial data even though gesture recognition accuracy was not perfect (*i.e.*, 0.945). This is due to the robust FSM-based gesture-to-instruction mapping that ensures the following transition rules:

- State-transitions are activated only if the corresponding gesture-tokens are detected for 15 consecutive frames.

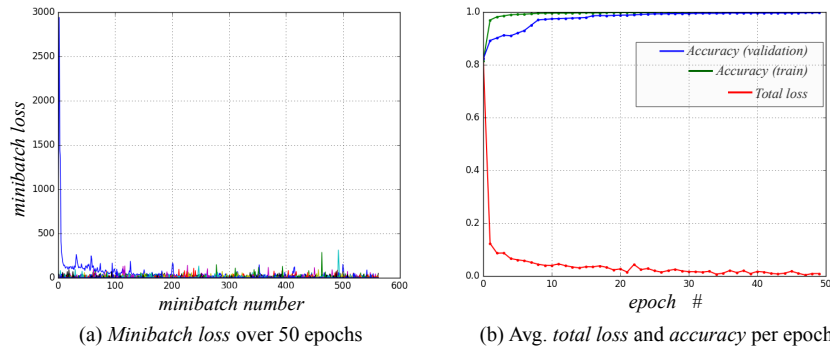


Figure 11: Training error and accuracy of our CNN model illustrated in Fig. 9. Training and validation sets contain 35K and 4K images, respectively; batch-size was set to 128 and the network was trained for 50 epoch.

- There are no transition rules (to other states) for incorrect gesture-tokens.

Consequently, an incorrect recognition has to happen 15 consecutive frames to generate an incorrect instruction, which is highly unlikely. However, in challenging visual conditions, region selection often fails to segment out the hand gestures correctly, which causes the overall process to fail. As the first row of Table 1 suggests, our framework fails in 6 test cases out of 30; we inspected the failed cases and found the following issues:

- Surface reflection and air bubbles often cause problems to the region selector. Although surface reflection is not common in deep water, suspended particles and limited visibility will be additional challenges in deep open-water scenarios.
- In some cases, diver’s hand(s) appeared in front of his face or partially appeared in the field-of-view. In these cases, only some part of the hand(s) appeared in the selected region which eventually caused the gesture recognizer to detect ‘1’s as ‘0’, or ‘pic’s as ‘1’s, etc.

4.3 Performance Evaluation through Gazebo Simulation

We also performed simulation experiments on controlling an Aqua robot [25] based on instructions generated from sequence of hand gestures performed by a person.

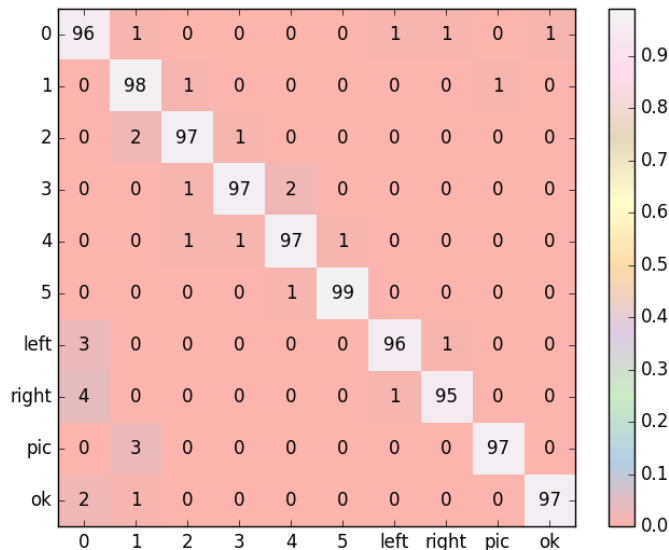


Figure 12: Confusion matrix based on test-set performance.

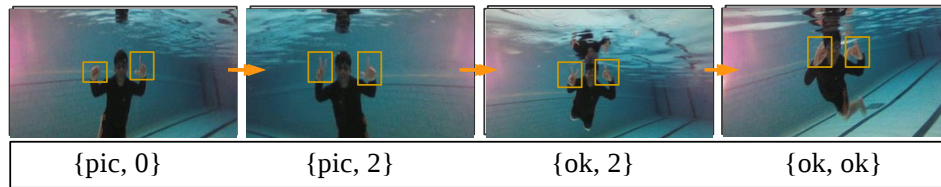
Table 1: Performance evaluation of our framework based on real-world data

Operating Medium	Total # of Instructions (Gestures)	Successfully Decoded	Accuracy (%)
Underwater	30 (162)	24 (128)	80 (78)
Terrestrial	20 (132)	20 (121)	100 (94.5)

The gesture sequences are captured through a webcam and the simulation is performed in Gazebo, on the ROS Kinetic platform [26]. As illustrated in Figure 14, gesture tokens are successfully decoded to control the robot. Although a noise-free simulation environment does not pose most challenges that are common in the real-world, it does help set benchmarks for expected performance bounds and is useful in human interaction studies, which is described in the following section.

4.4 Human Interaction Study

We performed a human interaction study where the participants are introduced to our hand gesture based framework, the fiducial-based RoboChat framework [1], and the RoboChat-Gesture framework [2] where a set of discrete motions from a pair of fiducials are interpreted as gesture-tokens. AprilTags [11] were used for the RoboChat trials to deliver commands.



STOP current-program, EXECUTE Program 2, GO.

Figure 13: Generating instructions from sequence of hand gestures performed by a diver

A total of ten individuals participated in the study, who were grouped according to their familiarity to robot programming paradigms in the following manner:

- Beginner: participants who are unfamiliar with gesture/fiducial based robot programming (2 participants)
- Medium: participants who are familiar with gesture/fiducial based robot programming (7 participants)
- Expert: participants who are familiar and practicing these frameworks for some time (1 participant)

In the first set of trials, participants are asked to perform sequences of gestures to generate the following instructions (Fig. 5) in all three interaction paradigms:

1. STOP current-program, HOVER for 50 seconds, GO.
2. CONTD current-program, take SNAPSHOTS for 20 seconds, GO.
3. CONTD current-program, Update Parameter 3 to DECREASE, GO.
4. STOP current-program, EXECUTE Program 1, GO.

The second set of trials, participants had to program the robot with complex instructions and were given the following two scenarios:

- a. *The robot has to stop its current task and execute program 2 while taking snapshots, and*
- b. *The robot has to take pictures for 50 seconds and then start following the user.*

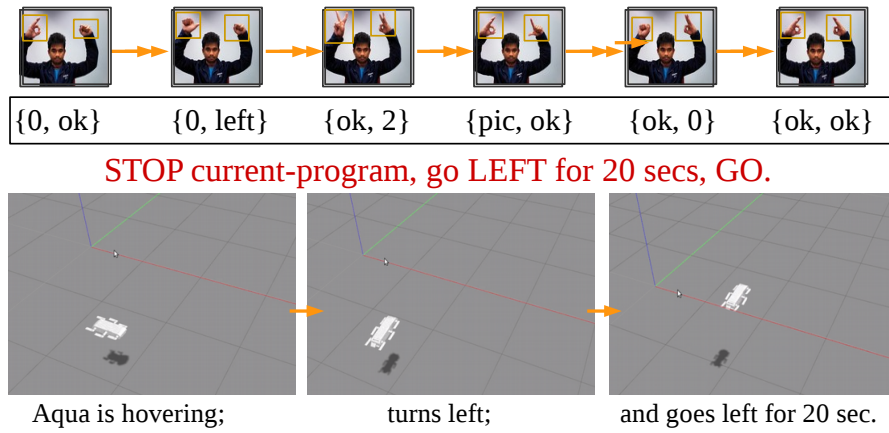


Figure 14: Controlling an Aqua robot based on instructions generated from sequence of hand gestures performed by a person; the simulation is performed in Gazebo, on ROS-kinetic platform [26].

For all the experiments mentioned above, participants performed gestures with hands, AprilTags, and discrete motions with AprilTags. Correctness and the amount of time taken were recorded in each case. Fig. 15 shows the comparisons of average time taken to perform gestures for generating different types of instructions. Participants quickly adopted the hand gestures to instruction mapping and took significantly less time to finish programming compared to the other two alternatives. Specifically, participants found it inconvenient and time consuming to search through all the tags for each instruction token. On the other hand, although performing a set of discrete motions with only two AprilTags saves time, it was less intuitive to the participants. As a result, it still took a long time to formulate the correct tokens for complex instructions, as evident from Fig. 15.

One interesting result is that the *beginner* users took less time to complete the instructions compared to *medium* users. This is probably due to the fact that unlike the beginner users, medium users were trying to intuitively interpret and learn the syntax while performing the gestures. However, as illustrated by Table 2, beginner users made more mistakes on an average before completing an instruction successfully. Expert user performed all tasks in the first try, hence comparison for beginner and medium users is presented only. Since there are no significant differences on number of mistakes for any types of user, we conclude that simplicity, efficiency, and intuitiveness are the major advantages of our framework over the existing methods.

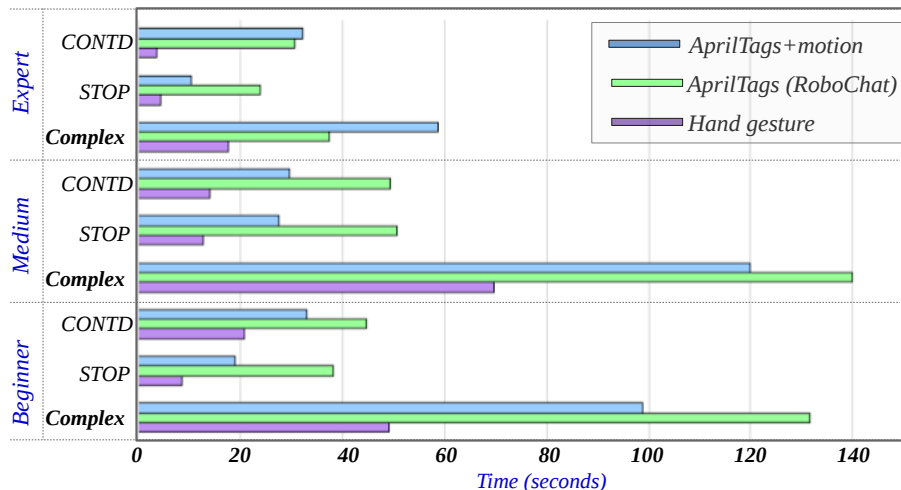


Figure 15: Comparisons of average time taken to perform gestures for successfully generating different types of programs (*STOP*: instruction 1 and 4, *CONTD*: instruction 2 and 3, *Complex*: scenario *a* and *b*).

5 Conclusions and Future Work

In this paper, we present a hand gesture based human-robot communication framework for underwater robots, where divers can use a set of intuitive and meaningful hand gestures to program new instructions for an accompanying robot or reconfigure existing program parameters on the fly. In the proposed framework, a CNN model provides accurate hand gesture recognition and a FSM-based deterministic model performs efficient gesture-to-instruction mapping. Accuracy and robustness of the framework is evaluated through extensive experiments, while an user interaction study is performed to evaluate the usability of the interface. Future work will investigate methods to accommodate a larger vocabulary of instructions and useful features such as control-flow tokens, while maintaining simplicity and robustness of the approach. In addition, work will focus on designing an improved and more robust region selector. A complete evaluation of the interaction framework through open-water trials is the immediate next step.

References

- [1] G. Dudek, J. Sattar, and A. Xu, "A visual language for robot control and programming: A human-interface study," in *2007 IEEE International Con-*

Table 2: Average number of mistakes using [*hand gesture, Robochat, AprilTags with motion*] for different users before correctly generating the instruction

Instruction Type	Total # of Instructions (Gestures)	Beginner User	Medium User
STOP	2 (10)	[2, 1, 3]	[1, 0, 1]
CONTD	2 (10)	[0, 0, 1]	[0, 0, 0]
Complex	2 (16)	[2, 3, 7]	[2, 2, 3]

ference on Robotics and Automation (ICRA), pp. 2507–2513, IEEE, 2007.

- [2] A. Xu, G. Dudek, and J. Sattar, “A natural gesture interface for operating robotic systems,” in *2008 IEEE International Conference on Robotics and Automation (ICRA)*, pp. 3557–3563, IEEE, 2008.
- [3] D. Chiarella, M. Bibuli, G. Bruzzone, M. Caccia, A. Ranieri, E. Zereik, L. Marconi, and P. Cutugno, “Gesture-based language for diver-robot underwater interaction,” in *OCEANS 2015-Genova*, pp. 1–9, IEEE, 2015.
- [4] G. Dudek, P. Giguere, and J. Sattar, “Sensor-based behavior control for an autonomous underwater vehicle,” in *Experimental Robotics*, pp. 267–276, Springer, 2008.
- [5] E. Coronado, J. Villalobos, B. Bruno, and F. Mastrogiovanni, “Gesture-based robot control: Design challenges and evaluation with humans,” in *2017 IEEE International Conference on Robotics and Automation (ICRA)*, pp. 2761–2767, IEEE, 2017.
- [6] S. Chen, H. Ma, C. Yang, and M. Fu, “Hand gesture based robot control system using leap motion,” in *International Conference on Intelligent Robotics and Applications*, pp. 581–591, Springer, 2015.
- [7] M. T. Wolf, C. Assad, M. T. Vernacchia, J. Fromm, and H. L. Jethani, “Gesture-based robot control with variable autonomy from the JPL BioSleeve,” in *2013 IEEE International Conference on Robotics and Automation (ICRA)*, pp. 1160–1165, IEEE, 2013.
- [8] M. Fiala, “ARTag, a fiducial marker system using digital techniques,” in *2005 IEEE Computer Society Conference on Computer Vision and Pattern Recognition (CVPR)*, vol. 2, pp. 590–596, IEEE, 2005.

- [9] M. Skubic, D. Perzanowski, S. Blisard, A. Schultz, W. Adams, M. Bugajska, and D. Brock, "Spatial language for human-robot dialogs," *IEEE Transactions on Systems, Man, and Cybernetics, Part C (Applications and Reviews)*, vol. 34, no. 2, pp. 154–167, 2004.
- [10] G. Dudek, M. Jenkin, C. Prahacs, A. Hogue, J. Sattar, P. Giguere, A. German, H. Liu, S. Saunderson, A. Ripsman, *et al.*, "A visually guided swimming robot," in *2005 IEEE/RSJ International Conference on Intelligent Robots and Systems (IROS)*, pp. 3604–3609, IEEE, 2005.
- [11] E. Olson, "AprilTag: A robust and flexible visual fiducial system," in *Robotics and Automation (ICRA), 2011 IEEE International Conference on*, pp. 3400–3407, IEEE, 2011.
- [12] PhotoModeler, "PhotoModeler Coded Targets Module." <http://www.photomodeler.com/index.html>. Accessed: 8-30-2017.
- [13] J. Sattar, E. Bourque, P. Giguere, and G. Dudek, "Fourier tags: Smoothly degradable fiducial markers for use in human-robot interaction," in *2007 Fourth Canadian Conference on Computer and Robot Vision (CRV)*, pp. 165–174, IEEE, 2007.
- [14] S. Waldherr, R. Romero, and S. Thrun, "A gesture based interface for human-robot interaction," *Autonomous Robots*, vol. 9, no. 2, pp. 151–173, 2000.
- [15] P. Molchanov, S. Gupta, K. Kim, and J. Kautz, "Hand gesture recognition with 3D convolutional neural networks," in *Proceedings of 2015 IEEE conference on computer vision and pattern recognition workshops*, pp. 1–7, 2015.
- [16] N. Neverova, C. Wolf, G. W. Taylor, and F. Nebout, "Multi-scale deep learning for gesture detection and localization," in *Workshop at the European conference on computer vision*, pp. 474–490, Springer, 2014.
- [17] J. Nagi, F. Ducatelle, G. A. Di Caro, D. Cireşan, U. Meier, A. Giusti, F. Nagi, J. Schmidhuber, and L. M. Gambardella, "Max-pooling convolutional neural networks for vision-based hand gesture recognition," in *2011 IEEE International Conference on Signal and Image Processing Applications (ICSIPA)*, pp. 342–347, IEEE, 2011.
- [18] F. Shkurti, W.-D. Chang, P. Henderson, M. J. Islam, J. C. G. Higuera, J. Li, T. Manderson, A. Xu, G. Dudek, and J. Sattar, "Underwater multi-robot conveying using visual tracking by detection," in *2017 IEEE/RSJ International Conference on Intelligent Robots and Systems (IROS)*, IEEE, 2017.

- [19] M. J. Islam and J. Sattar, "Mixed-domain biological motion tracking for underwater human-robot interaction," in *2017 IEEE International Conference on Robotics and Automation (ICRA)*, pp. 4457–4464, IEEE, 2017.
- [20] V. Oliveira and A. Conci, "Skin detection using HSV color space," in *H. Pedrini, & J. Marques de Carvalho, Workshops of Sibgrapi*, pp. 1–2, 2009.
- [21] H.-S. Yeo, B.-G. Lee, and H. Lim, "Hand tracking and gesture recognition system for human-computer interaction using low-cost hardware," *Multimedia Tools and Applications*, vol. 74, no. 8, pp. 2687–2715, 2015.
- [22] TensorFlow, "CNN model for CIFAR-10 data." http://www.tensorflow.org/tutorials/deep_cnn. Accessed: 8-30-2017.
- [23] M. Abadi, A. Agarwal, P. Barham, E. Brevdo, Z. Chen, C. Citro, G. S. Corrado, A. Davis, J. Dean, M. Devin, *et al.*, "Tensorflow: Large-scale machine learning on heterogeneous distributed systems," *arXiv preprint arXiv:1603.04467*, 2016.
- [24] O. CA, "OpenROV Underwater Drone 2.8." <https://www.openrov.com/products/openrov28/>. Accessed: 8-30-2017.
- [25] G. Dudek, P. Giguere, C. Prahacs, S. Saunderson, J. Sattar, L.-A. Torres-Mendez, M. Jenkin, A. German, A. Hogue, A. Ripsman, *et al.*, "Aqua: An amphibious autonomous robot," *Computer*, vol. 40, no. 1, 2007.
- [26] Gazebo, "Gazebo simulation on ROS." http://gazebosim.org/tutorials?tut=ros_overview. Accessed: 8-30-2017.